Tetrahedron 65 (2009) 9081–9085

Contents lists available at ScienceDirect

Tetrahedron

journal homepage: www.elsevier.com/locate/tet

Coordination-driven self-organization of switchable [2]rotaxane

Feng-Yuan Ji †, Liang-Liang Zhu †, Dong Zhang, Zhao-Fei Chen, He Tian *

Key Laboratory for Advanced Materials and Institute of Fine Chemicals, East China University of Science & Technology, Shanghai 200237, PR China

ARTICLE INFO

Article history:
Received 10 July 2009
Received in revised form 4 September 2009
Accepted 11 September 2009
Available online 15 September 2009

ABSTRACT

A bistable porphyrin-containing [2]rotaxane is synthesized with a shuttling benzylic-amide macrocycle mechanically locked onto the thread subunit by formations of H-bonds with two potential stations. This macrocycle comprises two pyridine groups, which would be easily coordinated with zinc porphyrin. The Zn(II) coordination of porphyrin moiety on the thread subunit, immediately followed by the coordination with pyridine groups on the macrocycle, leads to an intermolecular axle-macrocycle-type nanostructure. Moreover, the self-assembly way shows great difference from the two states of the rotaxane monomer: The coordination-driven self-organization of the *trans*-state **E2** leads to a network structure, whereas the *cis*-state **Z2** gives birth to an irregular assembly.

1. Introduction

The design and construction of new supramolecular architectures so as to develop multifunctional and innovative material is essential to the nanotechnology.[1] The research interest of supramolecular systems, such as rotaxane and pseudorotaxane, has been changing from investigation of the single molecule in solution to the study of regular ensemble on surface or interphase.[2] Thus far, some different prototypes of rotaxane system have been reported to construct ordered arrays, such as cross-linked,[3] dendritic[4] and main-chain-type polymerization.[5] Utilization of functional and switchable rotaxane monomer[6] as building blocks to construct ordered molecular frameworks, to obtain sophisticated integrations with large scale, multi-respondent and coordinative properties, however, will still be a long-term challenge.[7]

Benzylic-amide macrocycle based [2]rotaxane[8] is considered as an ideal candidate for developing the above-mentioned supramolecular nanostructures, because the thread subunit and the macrocycle are both able to be modified into a variety of functional moieties. A porphyrin containing fluorescent [2]rotaxane based on a benzylic-amide macrocycle was synthesized recently and its shuttling motion was thermo- and photo-controllable.[8b] In spite of the optical property of the porphyrin moiety itself, the coordination of porphyrin with zinc(II) ion or together with other ligands also attracts scientists' attention. In this paper, we describe a novel [2]rotaxane with a porphyrin moiety on the thread and two pyridine groups on the benzylic-amide macro-ring. Once the porphyrin moiety is coordinated with zinc(II) ion, it can interact with the pyridine groups of another rotaxane monomer via intermolecular metal coordination, leading to a charming self-organized rotaxane nanostructures. For the switchable property of this [2]rotaxane monomer, the self-assembly ways and the morphologies of the assembly show great differences from the two tunable states of the [2]rotaxane monomer.

2. Experimental part

The rotaxane **Z2** consists of a benzylic amide macrocycle and a thread with two potential H bonding stations—fumaramide group and succinic amide group. The macrocycle is locked by two bulky stoppers, free base porphyrin and fluorene entities (see Scheme 1). This molecular shuttle **Z2** was prepared in 25% yield from thread **Z1** and could be converted into **E2** by heating, which could also be turned back to **Z2** by irradiation at 254 nm. The macrocycle contains two pyridine groups, which can undergo coordination with many metal ions. After addition of Zn^{2+} to the solution of rotaxane **Z2**/**E2**, the central hydrogen atoms in porphyrin moiety of the rotaxane would be replaced by zinc. Thus the zinc porphyrin moiety of one rotaxane monomer would be axially connected to a pyridyl unit of another monomer. There are two symmetrical pyridyl on the two sides of the macrocycle, hence the self-assembled supramolecular structure extends to a large network.

2.1. Materials and characterizations

All reagents and solvents were used as supplied, unless stated otherwise. CH_2Cl_2 was distilled over CaH_2. DMF was dried over molecular sieves, triethylamine were distilled from KOH, and THF

* Corresponding author. Tel.: +86 21 64252756; fax: +86 21 64252288.
E-mail address: tianhe@ecust.edu.cn (H. Tian).
† F.-Y. Ji and L.-L. Zhu contributed equally to this work.

0040-4020/$ – see front matter © 2009 Elsevier Ltd. All rights reserved.
doi:10.1016/j.tet.2009.09.051

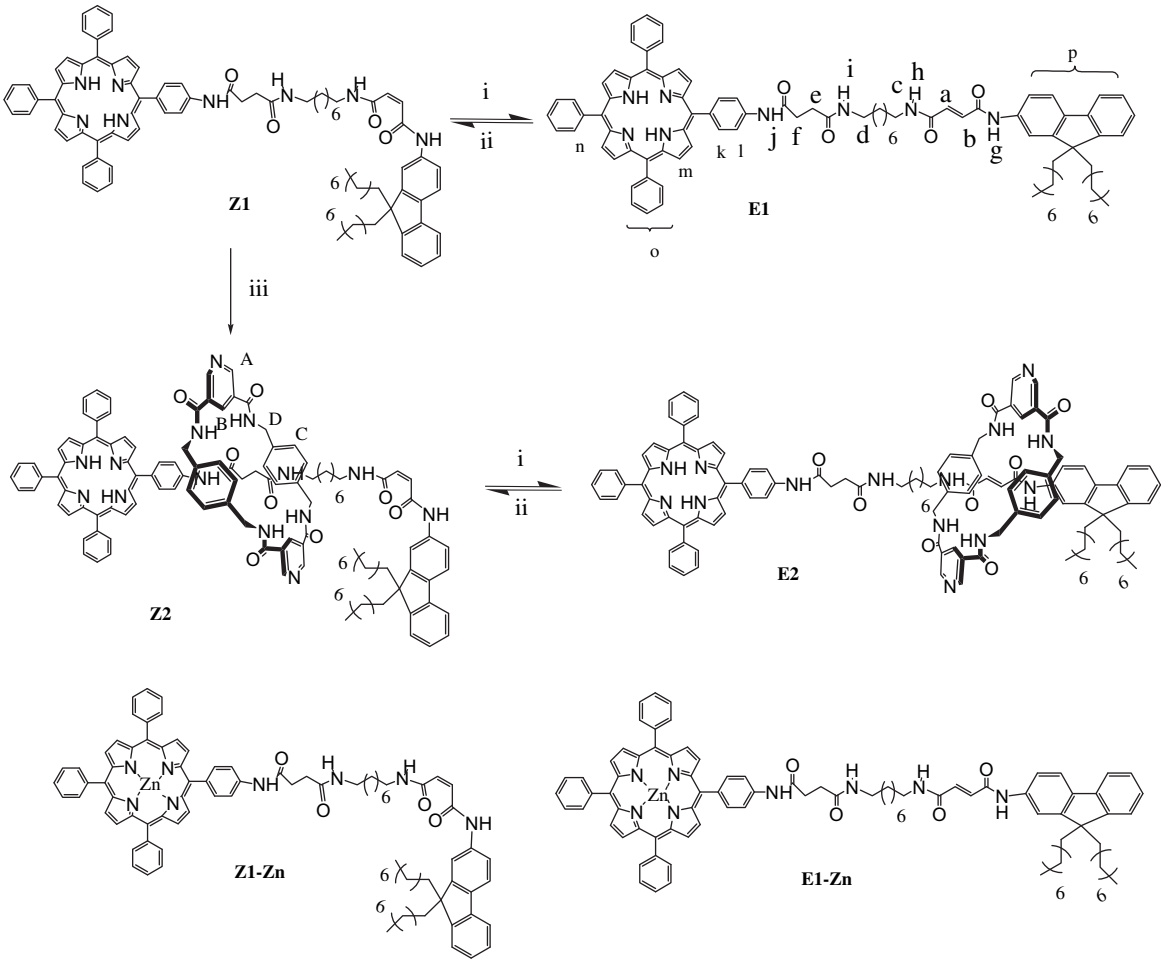

Scheme 1. Synthesis of bistable rotaxane **Z2**/**E2**. (i) 400 K, 51/49 for **E1**/**Z1** and 43/57 for **E2**/**Z2** in 1,1,2,2-tetra-chloride ethylene; (ii) 254 nm, 25/75 for **E1**/**Z1** and 18/82 for **E2**/**Z2** in CH_2Cl_2; (iii) *para*-xylylene diamine, 3,5-pyridinedicarbonyl dichloride, $Et_3N/CHCl_3$, 0 °C, 25%.

was distilled over sodium. MALDI-TOF mass spectra were recorded on a Brüker Biflex IV spectrometer. Flash column chromatography was performed on silica gel. ^1H NMR and ^{13}C NMR were measured on a Brüker AV-400, or AV-500 spectrometer with tetramethylsilane (TMS) as internal standard at 298 K. Elemental analysis was performed on a vario EL III instrument. Absorption spectra were done on a Varian Cary 500 UV/Vis spectrophotometer (1 cm quartz cell used). Fluorescent spectra were recorded on a Varian Cary Eclipse fluorescence spectrophotometer at 25 °C. The photo-irradiation was carried on a CHF-XM 500-W high-pressure mercury lamp with a filter for 254 nm in a sealed Ar-saturated 1 cm quartz cell. The scanning electron microscopy (SEM) was tested on JEOL (JSM-6360LV) electron microscope.

2.2. Synthesis of rotaxane Z2

The thread **Z1**[8b] (80 mg, 0.060 mmol) and Et_3N (61.6 mg, 1.440 mmol) in anhydrous $CHCl_3$ (100 mL) were stirred vigorously whilst solutions of *para*-xylylene diamine (97.92 mg, 0.720 mmol) in anhydrous $CHCl_3$ (40 mL) and 3,5-pyridinedicarbonyl dichloride (155.52 mg, 0.720 mmol) in anhydrous $CHCl_3$ (40 mL) were simultaneously added over a period of 2 h using motor-driven syringe pumps. After a further 2 h the resulting suspension was filtered and the solvent removed under reduced pressure. The resulting solid was subjected to column chromatography (silica gel) to yield unconsumed thread and [2]rotaxane **Z2** (yield=25%). Mp 175–177 °C. ^1H NMR (400 MHz, $CDCl_3/CD_3OD$=10/1): 11.80 (s, 1H, Hg), 9.70 (s, 1H, Hh), 9.24 (d, 4H, HA), 8.83–8.77 (m, 8H, pyrrole Hm), 8.73 (d, 2H, HB), 8.25 (m, 2H, Hk), 8.15 (m, 6H, *ortho* triphenyl Hn), 8.10 (d, 2H, 4-amino-phenyl, Hl), 7.79 (m, 3H, fluorene, Hp), 7.78–7.70 (m, 9H, *meta*/*para* triphenyl, Ho), 7.70–7.50 (m, 4H, fluorene, Hp), 7.23 (S, 8H, HC), 5.95–6.12 (d, 2H, Ha, Hb), 4.50–4.68 (br, 8H, HD), 3.20 (br, 2H, Hc), 2.95 (br, 2H, Hd), 2.00–2.40 (br, 4H, He, Hf), 1.90–0.50 (m, 46H, alkyl chain), −2.84 (s, 2H, pyrrole NH). MS: 1877.1 $[M+H]^+$. Elemental analysis calcd for **Z2** $(C_{119}H_{122}N_{14}O_8)(H_2O)_{26}$: C 60.97, H 7.42, N 8.37; found: C 60.90, H 7.28, N 8.15.

2.3. Synthesis of rotaxane E2

Rotaxane **E2** was obtained by the thermal isomerization of rotaxane **Z2**. The procedure was carried out as follows: **Z2** (15 mg, 0.008 mmol) was heated to 400 K in 1,1,2,2-tetra-chloride ethylene for 24 h. After cooling, **E2** and the unchanged **Z2** were separated and collected by chromatography (silica gel, first CH_2Cl_2, then $MeOH/CH_2Cl_2$=1/40), **E2** was obtained in a yield of 43%. Mp 180–182 °C. ^1H NMR (400 MHz, $CDCl_3$): 10.13 (s, 1H, Hg), 10.01 (s, 1H, Hh), 9.28 (d, 4H, HA), 8.95 (d, 2H, HB), 8.75–8.90 (m, 8H, pyrrole, Hm), 8.18–8.24 (m, 6H, *ortho* triphenyl Hn), 8.17 (m, 2H, Hk), 8.15 (d, 2H, 4-amino-phenyl, Hl), 7.98 (m, 3H, fluorene, Hp), 7.78–7.70 (m, 9H, *meta*/*para* triphenyl, Ho), 7.60–7.45 (m, 4H, fluorene, Hp), 7.10 (S, 8H, HC), 6.05–6.15 (d, 2H, Ha, Hb), 4.38–4.45 (br, 8H, HD), 3.20 (br, 2H, Hc), 3.06 (br, 2H, Hd), 2.60 (br, 2H, He), 2.49 (br, 2H, Hf), 1.95–0.50 (m, 46H, alkyl chain), −2.84 (s, 2H, pyrrole NH). MS: 1899.1 $[M+Na]^+$. Elemental analysis calcd for **E2** $(C_{119}H_{122}N_{14}O_8)(H_2O)_3$: C 74.06, H 6.64, N 10.16; found: C 73.99, H 6.78, N 9.82.

2.4. Photoisomerization procedures of rotaxane E2

Photoisomerization procedure of rotaxane **E2** was carried out as follows: Rotaxane **E2** was dissolved in CH_2Cl_2 (20 mL) in a quartz vessel. The solution was directly irradiated at 254 nm using a multi-lamp photo-reactor for 4 h. After the photostationary state was reached the reaction mixture was concentrated under reduced pressure to afford the crude product, then re-dissolved in CH_2Cl_2 and washed with satd Na_2CO_3 prior to purification by column chromatography. 18% percent of **E2** were converted to **Z2**.

2.5. Z2-Zn-Complex

The rotaxane **Z2** (10 mg, 0.0053 mmol) in anhydrous $CHCl_3$ were stirred vigorously whilst the zinc acetate (3.88 mg, 0.060 mmol) were added. This mixture was stirred overnight at room temperature. The resulting solution was washed with brine (2×25 mL), water, the organic layer was dried over $MgSO_4$ and the liquid evaporated to dryness under reduced pressure to obtain the pure compound in quantitative yield. Mp 192–194 °C. ^{1}H NMR (400 MHz, $CDCl_3/CD_3OD$=10/1): 11.58 (s, 1H, Hg), 9.52 (s, 1H, Hh), 8.80–8.90 (m, 8H, pyrrole Hm), 8.34 (m, 2H, Hk), 8.18–8.22 (m, 6H, *ortho* triphenyl Hn), 8.18 (d, 2H, 4-amino-phenyl, Hl), 7.95 (s, 2H, HB), 7.75–7.80 (m, 9H, *meta*/*para* triphenyl, Ho), 7.42–7.63 (m, 7H, fluorene, Hp), 7.06 (S, 8H, HC), 5.82–5.95 (d, 2H, Ha, Hb), 4.25–4.48 (br, 8H, HD), 3.13–3.65(m, 4H, Hc, Hd, He, Hf), 2.84 (br, 4H, HA), 1.95–0.50(m, 46H, alkyl chain). Elemental analysis calcd for **Z2-Zn-Complex** $(C_{119}H_{120}N_{14}O_8Zn)(H_2O)_{31}$: C 57.23, H 7.29, N 7.85; found: C 57.17, H 7.26, N 7.56.

2.6. E2-Zn-Complex

This compound was prepared as described above. Mp 196–197 °C. ^{1}H NMR (400 MHz, $CDCl_3$): 9.60 (s, 1H, Hg), 9.59 (s, 1H, Hh), 8.90–8.83 (m, 8H, pyrrole Hm), 8.40 (m, 2H, Hk), 8.15–8.32 (m, 6H, *ortho* triphenyl Hn), 8.10 (d, 2H, 4-amino-phenyl, Hl), 7.88 (s, 2H, HB), 7.70–7.60 (m, 9H, *meta*/*para* triphenyl, Ho), 7.60–7.30 (m, 7H, fluorene, Hp), 6.83 (S, 8H, HC), 5.82–5.56 (d, 2H, Ha, Hb), 4.35–4.02 (br, 8H, HD), 3.01–2.82 (m, Hc, Hd, He, Hf), 2.70 (br, 4H, HA), 2.05–0.50 (m, 46H, alkyl chain). Elemental analysis calcd for **E2-Zn-Complex** $(C_{119}H_{120}N_{14}O_8Zn)(H_2O)_{47}$: C 51.31, H 7.68, N 7.04; found: C 51.16, H 7.46, N 6.99.

3. Results and discussion

The detailed structure of **Z2** and **E2** were confirmed by ^{1}H NMR spectra. The ^{1}H NMR spectra of **E1**/**Z1**, **E2**/**Z2** and their coordinated species in $CDCl_3$ are shown in Figure 1. The assignment of these proton signals is based on our previous report and other relevant literatures about benzylic-amide macrocycle based [2]rotaxane.[8,9] The chemical shifts of Ha and Hb protons of fumaramide group in rotaxane **E2** were shielded and revealed upfield shifts of up to −1.12 and −1.00 ppm, respectively, compared with those of the thread **E1**, whereas Hg and Hh displayed downfield shifts of up to 0.48 and 0.31 ppm. These proton signals change was originated from benzylic-amide macrocycle fixing on the thread subunit. On the other hand, the He and Hf protons of succinic amide group resonated at almost identical shifts in both compounds (see Fig. 1a and b), indicating the macrocycle located in fumaramide group in rotaxane **E2**. The ^{1}H NMR variation situation in rotaxane **Z2** was just reversed. The chemical shifts of Ha, Hb protons didn't show too much difference between rotaxane **Z2** and thread **Z1**, but He and Hf protons were shielded by xylylene rings and revealed upfield shifts of up to −0.67 and −0.51 ppm, respectively, in rotaxane **Z2** (see Fig. 1d and e). These spectral changes confirmed that the macrocycle would shuttle from the fumaramide station to the succinic amide moiety,

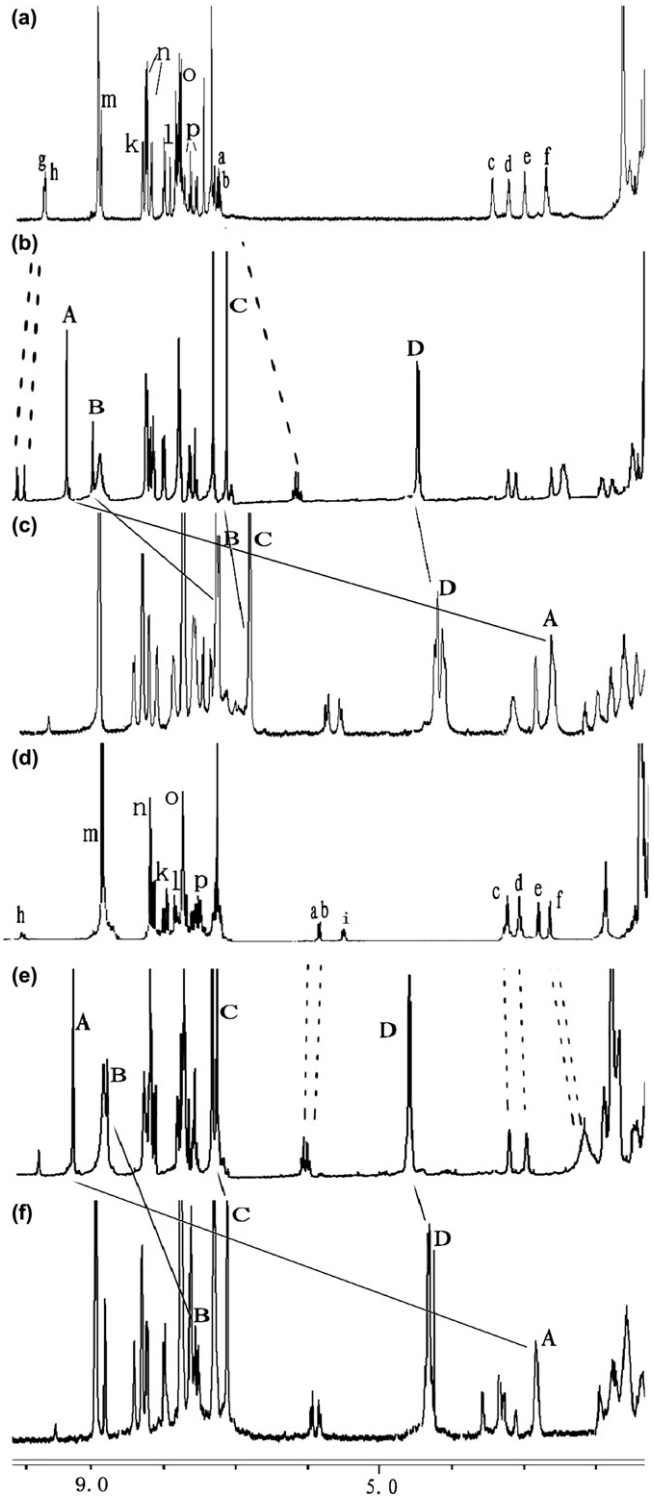

Figure 1. ^{1}H NMR (400 MHz, a–c in $CDCl_3$, d–f in $CDCl_3/CD_3OD$=10/1) of (a) thread **E1**, (b) rotaxane **E2**, (c) **E2-Zn-Complex**, (d) thread **Z1**, (e) rotaxane **Z2**, (f) **Z2-Zn-Complex**.

accompanied by the conformational change of the interlocked supramolecule from rotaxane **E2** to **Z2**.[9] After replacing hydrogen atoms of porphyrin moiety by zinc ion, the ^{1}H NMR signals of **E2-Zn-Complex** and **Z2-Zn-Complex** became broad and the spectra showed great difference compared with their corresponding monomers (see Fig. 1c and f). All the protons of the benzylic amide macrocycle, especially the protons HA on the pyridine groups, shifted to the upfield significantly because of the great shielding effects of zinc porphyrin, which the macrocycle ring sticks to. These

changes confirmed that the stopper zinc porphyrin of one rotaxane monomer was axially connected to pyridyl unit of another.[10]

We have also investigated into the optical properties of **E2-Zn-Complex** and **Z2-Zn-Complex**, compared with their reference threads **E1-zn**/**Z1-zn**. The absorption spectra of **E1-zn**/**Z1-zn** display a typical intense Soret bands at 424 nm and Q bands at 551 nm. However, the maximum absorption of **E2-Zn-Complex** and **Z2-Zn-Complex** shows a red shift compared with their references, respectively. The phenomena are coincident with the ones described in related reports, i.e., on axial coordination of pyridyl residues, the absorption bands of zinc porphyrin display a red shift up to some nanometers (Fig. 2a and b).[11]

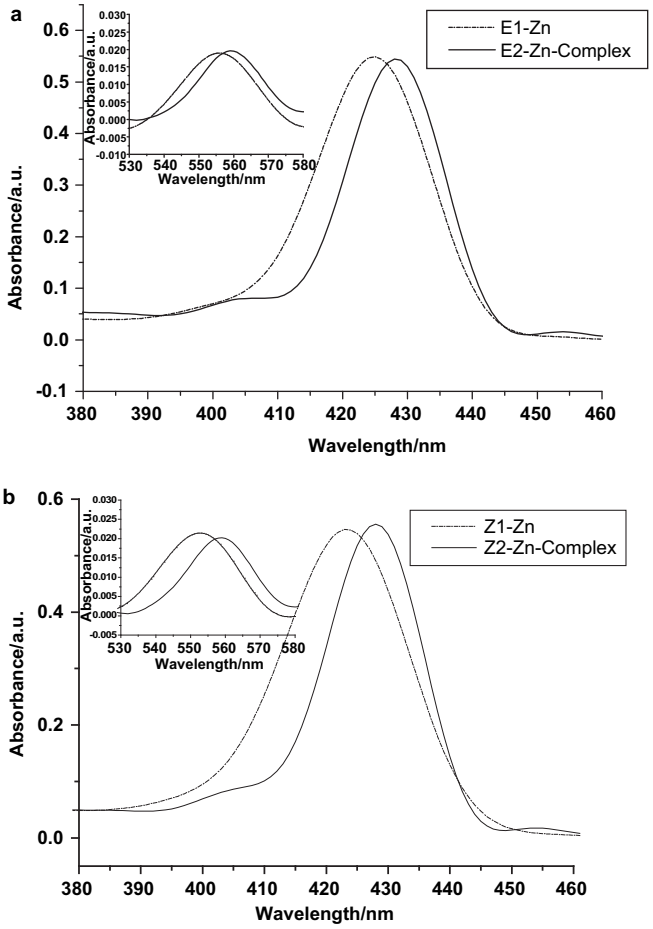

Figure 2. (a) UV–vis spectra of **E2-Zn-Complex** and reference **E1-Zn** in CH_2Cl_2 (c=3×10^{-5} M). (b) UV–vis spectra of **Z2-Zn-Complex** and reference **Z1-Zn** in CH_2Cl_2 (c=3×10^{-5} M).The insets show the corresponding Q-band absorptions.

The emission of CH_2Cl_2 solution of metalized rotaxane **E2**/**Z2** assemblies and their references **E1-zinc**/**Z1-zinc** (isosbestic point of metalized rotaxane assembly and reference threads) are shown in Figure 3. It is interesting that the fluorescence emission of metalized **E2**/**Z2** assemblies also red shifted as compared with **E1-zinc**/**Z1-zinc**, because of the formation of self-assemblies from the rotaxane monomers. And it is notable that the assembled rotaxane **Z2** displays much stronger fluorescence than **Z1-zinc** (see Fig. 3b). It is suggested that **Z1-zinc**'s fluorescence is weakened due to its intermolecular π–π stacking of porphyrin zinc(II) moieties. However, the π–π stacking of porphyrin parts were eliminated, when the porphyrin zinc(II) segments were mainly axially coordinated to pyridyl residues by the complexation effect, so that the fluorescence became strong.

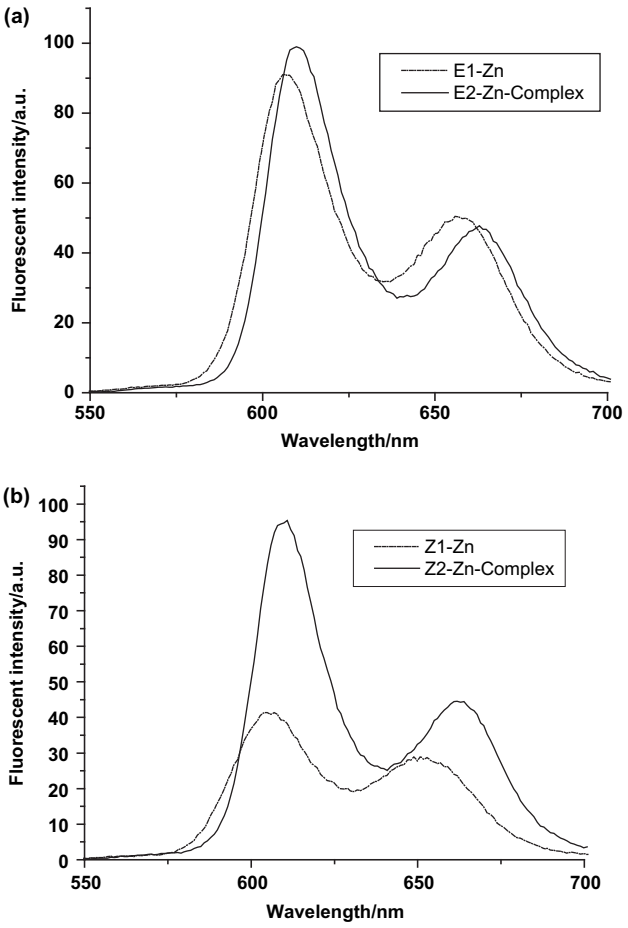

Figure 3. (a) Fluorescence emission spectra (λ_{exc}=427 nm, c=3×10^{-5} M) of **E2-Zn-Complex** and reference **E1-Zn** in CH_2Cl_2. (b) Fluorescence emission spectra (λ_{exc}=427 nm, c=3×10^{-5} M) of **Z2-Zn-Complex** and reference **Z1-Zn** in CH_2Cl_2.

Interior morphologies of metalized rotaxane **E2** and **Z2** assemblies were studied in terms of scanning electric microscopy (SEM). The leaner rotaxane monomer **E2** could be self-aggregated to some extend, forming rod structures observed in Figure 4A. On the other hand, annular structures were formed by the self-aggregation of curly monomer **Z2** (see Fig. 4C). This information reveals the different conformations of the two isomers of the rotaxane will lead to obviously self-aggregated structures, which may be caused by intermolecular H–H bonding and the π–π stacking of the chromophores at the two sides of the thread subunit. The coordination-driven self-organization process of the rotaxane monomers has taken place after mixing zinc(II) ion with the rotaxane in a 1:1 M ratio, which corresponds to the building of the axle-macrocycle-type nanostructures. Figure 4B shows the SEM image of the self-organization of rotaxane **E2** (**E2-Zn-Complex**) obtained after the metal coordination occurred. A regular formed network can be clearly observed. The average size of single annular cavity is about 120 nm in diameter, while the width of the edge of the hole is estimated to be around 20 nm, observed from SEM. However, the metalized rotaxane **Z2** was organized in a different way as that did in the situation of **E2**. Figure 4D shows the SEM images of rotaxane **Z2** after the metalization happening (**Z2-Zn-Complex**), an irregular assembly rather than the networks. The self-organized morphology is an enlarged result, which also reflect the greatly influence of the conformational structures of rotaxane monomers on the integrative morphology of the nanostructure resulted by the axle-macrocycle-type coordination procedure. Anyway, the linear **E2** is prone to form slight networks while the curly structural **Z2** leads to block structures.

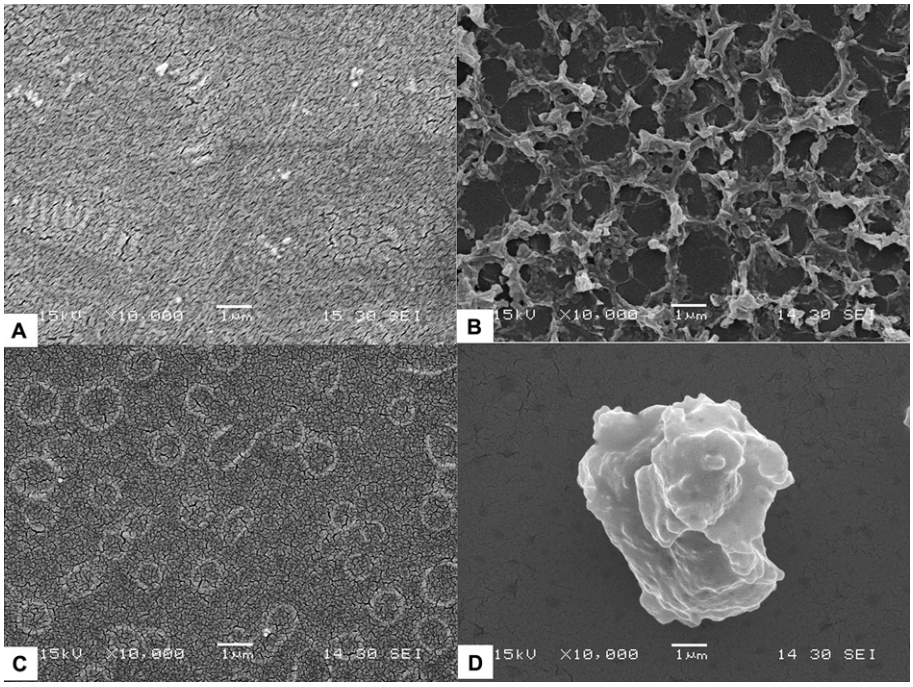

Figure 4. Scanning electron micrograph of the rotaxane **E2** before (A) and after (B) metalization by adding zinc acetate; **Z2** before (C) and after (D) metalization by adding zinc acetate.

4. Conclusions

A new bistable [2]rotaxane, with a porphyrin-containing thread subunit and two pyridine groups bearing macrocycle, has been demonstrated. The metalization of both the two states of the rotaxane monomer leads to intermolecular axle-macrocycle-type coordination with ultimately formations into different morphologies of rotaxane assemblies. The ^{1}H NMR spectral changes and the UV–vis spectra confirmed the metal coordination procedure of the switchable rotaxane before and after the aggregations occurred, and the SEM spectroscopic images of the metalized rotaxane film demonstrated the formations of the rotaxane nanostructures. Interestingly, the *trans*-rotaxane state **E2** formed the network structure while the *cis*- one **Z2** gave an irregular assembly after the metalization. Investigations of the detailed morphology of the rotaxane nanostructures and the mechanism that the different ways in which the *E*/*Z* states of the rotaxane aggregate are now under way.

Acknowledgements

This work was supported by NSFC/ China (50673025, 20603009), National Basic Research 973 Program (2006CB806200) and Scientific Committee of Shanghai.

Supplementary data

Experimental procedure and characterization for reference compounds **E1-Zn** and **Z1-Zn**, ^{1}H NMR spectra of **E1-Zn** and **Z1-Zn**, MALDI-TOF MS spectra of rotaxane **E2** and **Z2** are available free of charge via the online version. Supplementary data associated with this article can be found in online version at doi:10.1016/j.tet.2009.09.051.

References and notes

1. (a) Blanco, M.-J.; Jiménez, M. C.; Chambron, J.-C.; Heitz, V.; Linke, M.; Sauvage, J.-P. *Chem. Soc. Rev.* **1999**, *28*, 293–305; (b) Willner, I.; Basnar, B.; Willner, B. *Adv. Funct. Mater.* **2007**, *17*, 702–717; (c) Browne, W. R.; Feringa, B. L. *Nat. Nanotechnol.* **2006**, *1*, 25–35; (d) Pease, A. R.; Jeppesen, J. O.; Stoddart, J. F.; Luo, Y.; Collier, C. P.; Heath, J. R. *Acc. Chem. Res.* **2001**, *34*, 433–444; (e) Tian, H.; Wang, Q. C. *Chem. Soc. Rev.* **2006**, *35*, 361–374; (f) Wang, F.; Han, C.; He, C.; Zhou, Q.; Zhang, J.; Wang, C.; Li, N.; Huang, F. *J. Am. Chem. Soc.* **2008**, *130*, 11254–11255; (g) Zhu, L.-L.; Li, X.; Ji, F. Y.; Ma, X.; Wang, Q. C.; Tian, H. *Langmuir* **2009**, *25*, 3482–3486; (h) Amendola, V.; Dallacosta, C.; Fabbrizzi, L.; Monzani, E. *Tetrahedron* **2008**, *64*, 8318–8323.
2. (a) Stoddart, J. F. *Nat. Chem.* **2009**, *1*, 14–15; (b) Balzani, V.; Credi, A.; Venturi, M. *ChemPhysChem* **2008**, *9*, 202–220; (c) Moulin, J.-F.; Kengne, J. C.; Kshirsagar, R.; Cavallini, M.; Biscarini, F.; León, S.; Zerbetto, F.; Bottari, G.; Leigh, D. A. *J. Am. Chem. Soc.* **2006**, *128*, 526–532; (d) Liu, Y.; Liang, P.; Chen, Y.; Zhang, Y.-M.; Zheng, J.-Y.; Yue, H. *Macromolecules* **2005**, *38*, 9095–9099.
3. Bilig, T.; Oku, T.; Furusho, Y.; Koyama, Y.; Asai, S.; Takata, T. *Macromolecules* **2008**, *41*, 8496–8503.
4. Alvarez-Parrilla, E.; Cabrer, P. R.; Al-Soufi, W.; Meijide, F.; Nunez, E. R.; Tato, J. V. *Angew. Chem., Int. Ed.* **2000**, *39*, 2856–2858.
5. Sato, T.; Takata, T. *Macromolecules* **2008**, *41*, 2739–2742.
6. (a) Qu, D. H.; Wang, Q. C.; Tian, H. *Angew. Chem., Int. Ed.* **2005**, *44*, 5296–5299; (b) Klotz, E. J. F.; Claridge, T. D. W.; Anderson, H. L. *J. Am. Chem. Soc.* **2006**, *128*, 15374–15375; (c) Zhu, L.; Ma, X.; Ji, F.; Wang, Q.; Tian, H. *Chem.—Eur. J.* **2007**, *13*, 9216–9222; (d) Nygaard, S.; Leung, K. C. F.; Aprahamian, I.; Ikeda, T.; Saha, S.; Laursen, B. W.; Kim, S. Y.; Hansen, S. W.; Stein, P. C.; Flood, A. H.; Stoddart, J. F.; Jeppesen, J. O. *J. Am. Chem. Soc.* **2007**, *129*, 960–970; (e) Zhao, X.; Jiang, X.-K.; Shi, M.; Yu, Y.-H.; Xia, W.; Li, Z.-T. *J. Org. Chem.* **2001**, *66*, 7035–7043.
7. (a) Yaghi, O. M.; O'Keeffe, M.; Ockwig, N. W.; Chae, H. K.; Eddaoudi, M.; Kim, J. *Nature* **2003**, *433*, 705–714; (b) Gibson, H. W.; Nagvekar, D. S.; Yamaguchi, N.; Bhattarcharjee, S.; Wang, H.; Vergne, M.; Hercules, D. M. *Macromolecules* **2004**, *37*, 7514–7529.
8. (a) Pérez, E. M.; Dryden, D. T. F.; Leigh, D. A.; Teobaldi, G.; Zerbetto, F. *J. Am. Chem. Soc.* **2004**, *126*, 12210–12211; (b) Ji, F.-Y.; Zhu, L.-L.; Ma, X.; Wang, Q.-C.; Tian, H. *Tetrahedron Lett.* **2009**, *50*, 597–600.
9. (a) Li, Y.; Li, H.; Li, Y.; Liu, H.; Wang, S.; He, X.; Wang, N.; Zhu, D. *Org. Lett.* **2005**, *7*, 4835–4838; (b) Altieri, A.; Bottari, G.; Dehez, F.; Leigh, D. A.; Wong, J. K. Y.; Zerbetto, F. *Angew. Chem., Int. Ed.* **2003**, *42*, 2296–2300.
10. (a) Xiao, X.; Xu, W.; Zhang, D.; Xu, H.; Lu, H.; Zhu, D. *J. Mater. Chem.* **2005**, *15*, 2557–2561; (b) Muraoka, T.; Kinbara, K.; Aida, T. *Nature* **2006**, *440*, 512–515.
11. (a) Frey, J.; Tock, C.; Collin, J.-P.; Heitz, V.; Sauvage, J.-P. *J. Am. Chem. Soc.* **2008**, *130*, 4592–4593; (b) Borovkov, V. V.; Hembury, G. A.; Inoue, Y. *Acc. Chem. Res.* **2004**, *37*, 449–459.